Chinese Journal of Physiology 61(4): 221-229, 2018
DOI: 10.4077/CJP.2018.BAH594

Effect of Captopril on Ca^{2+} Homeostasis and Cell Viability in Human Hepatoma Cells

I-Shu Chen[1, *], Chiang-Ting Chou[2], Wei-Zhe Liang[3, 4, 5, *], Yuan-Yuarn Liu[6, *] Chun-Chi Kuo[7], Jue-Long Wang[8], Lyh-Jyh Hao[9], and Chung-Ren Jan[3]

[1]Department of Surgery, Kaohsiung Veterans General Hospital, Kaohsiung 81362
[2]Department of Nursing, Division of Basic Medical Sciences, Chang Gung University of Science and Technology, Chia-Yi 61363
[3]Department of Medical Education and Research, Kaohsiung Veterans General Hospital Kaohsiung 81362
[4]Department of Pharmacy, Tajen University, Pingtung 90741
[5]Yuh-Ing Junior College of Health Care & Management, Kaohsiung 80776
[6]Division of Trauma, Department of Emergency, Kaohsiung Veterans General Hospital Kaohsiung 81362
[7]Department of Nursing, Tzu Hui Institute of Technology, Pingtung 92641
[8]Department of Rehabilitation, Kaohsiung Veterans General Hospital Tainan Branch, Tainan 71051 and
[9]Department of Metabolism, Kaohsiung Veterans General Hospital Tainan Branch, Tainan 71051, Taiwan, Republic of China

Abstract

Captopril, an angiotensin-converting enzyme (ACE) inhibitor, induced different Ca^{2+} signaling responses in various cell models. However, the effect of captopril on Ca^{2+} homeostasis and cell viability in hepatoma cells is unknown. This study examined whether captopril altered Ca^{2+} homeostasis and viability in HepG2 human hepatoma cells. Intracellular Ca^{2+} concentrations in suspended cells were monitored by using the fluorescent Ca^{2+}-sensitive dye fura-2. Cell viability was examined by using 4-[3-[4-Iodophenyl]-2-4(4-nitrophenyl)-2H-5-tetrazolio-1,3-benzene disulfonate] water soluble tetrazolium-1 (WST-1). Captopril at concentrations of 500-3000 μM induced cytosolic free concentrations of Ca^{2+} ($[Ca^{2+}]_i$) rises in a concentration-dependent manner. Ca^{2+} removal reduced the signal by approximately 15%. Mn^{2+} has been shown to enter cells through similar mechanisms as Ca^{2+} but quenches fura-2 fluorescence at all excitation wavelengths. Captopril (3000 μM)-induced Mn^{2+} influx indirectly suggested that captopril evoked Ca^{2+} entry. Captopril-induced Ca^{2+} entry was inhibited by 15% by a protein kinase C (PKC) activator (phorbol 12-myristate 13 acetate, PMA) and an inhibitor (GF109203X) and three inhibitors of store-operated Ca^{2+} channels: nifedipine, econazole and SKF96365. In Ca^{2+}-free medium, treatment with the endoplasmic reticulum Ca^{2+} pump inhibitor 2,5-di-tert-butylhydroquinone (BHQ) abolished captopril-evoked $[Ca^{2+}]_i$ rises. Conversely, treatment with captopril abolished BHQ-evoked $[Ca^{2+}]_i$ rises. Inhibition of phospholipase C (PLC) with U73122 inhibited 70% of captopril-induced $[Ca^{2+}]_i$ rises. Captopril at concentrations between 150-550 μM killed cells in a concentration-dependent fashion. Chelation of cytosolic Ca^{2+} with 1,2-bis(2-aminophenoxy)ethane-N,N,N',N'-tetraacetic acid/acetoxy methyl (BAPTA/AM) did not reverse captopril's cytotoxicity. Together, in HepG2 human hepatoma cells, captopril induced $[Ca^{2+}]_i$ rises

Corresponding authors: [1] Jue-Long Wang, Department of Rehabilitation, Kaohsiung Veterans General Hospital Tainan Branch, Tainan 71051, Taiwan, ROC; [2] Lyh-Jyh Hao, Department of Metabolism, Kaohsiung Veterans General Hospital Tainan Branch, Tainan 71051, Taiwan, ROC; and [3] Chung-Ren Jan, Department of Medical Education and Research, Kaohsiung Veterans General Hospital, Kaohsiung, 81362, Taiwan, ROC. Tel: +886-7-3422121 ext.1509. Fax: +886-7-3468056. E-mail: crjan@isca.vghks.gov.tw.
*Contributed equally to this work.
Received: January 22, 2018; Revised: August 9, 2018; Accepted: August 17, 2018.
 ISSN : 0304-4920. http://www.cps.org.tw

and caused cell death that was not triggered by preceding $[Ca^{2+}]_i$ rises.

Key Words: Ca^{2+}, captopril, endoplasmic reticulum, human hepatoma cells, viability

Introduction

Angiotensin-converting enzyme (ACE) inhibitors contribute greatly to the cardiovascular field. Captopril is a widely used ACE inhibitor for treating blood pressure-related disorders (26). Regarding cardiovascular research, captopril was shown to reverse the adverse cardiovascular effects of polymerized hemoglobin (22) and counteract angiotensin II-mediated endothelial cell dysfunction by modulating the p38/SirT1 axis (24). Additionally, captopril has been shown to induce protective or cytotoxic effects on different cell models. On the aspect of protective effects, captopril inhibited neutrophil-dependent cytotoxicity in human endothelial cells (1), prevented meconium-induced cytokine expression and death in human lung cells (42), and attenuated oxidative stress-induced endothelial cell death (40). Conversely, captopril is a potential inhibitor of lung tumor growth and metastasis (2) and induced cytotoxicity in human leukemic cells (9). However, the effect of captopril on Ca^{2+}-related physiology in human hepatoma cells is still unclear.

A rise in cytosolic free concentrations of Ca^{2+} ($[Ca^{2+}]_i$) plays a crucial role in triggering and regulating diverse cellular responses including proliferation, apoptosis, secretion, contraction, protein activation, gene expression, *etc.* (3). This Ca^{2+} signaling is composed of Ca^{2+} influx from extracellular medium and Ca^{2+} release from organelles, and is precisely regulated by various signaling pathways (13). In non-excitable cells such as hepatocytes, it has been shown that the main pathway of Ca^{2+} influx is the store-operated Ca^{2+} influx and the main internal Ca^{2+} store is the endoplasmic reticulum Ca^{2+} store (28).

The effects of captopril on Ca^{2+} signaling have been studied in different models. It has been shown that captopril decreased intracellular Ca^{2+} content in isolated rat cardiomyocytes (36) and reduced vasoconstriction and Ca^{2+} fluxes in aortic smooth muscle (43, 44), but enhanced bradykinin-induced Ca^{2+} transients in cultured bovine aorta endothelial cells (18). Although captopril evoked different Ca^{2+} responses in various models, the effect of captopril on hepatoma cells is unknown. In order to understand the physiological significance of a Ca^{2+} signal, it is important to elucidate the mechanisms underlying the signal.

A previous study has shown that captopril has antifibrosis effects on hepatic fibrosis development in rats (37). Therefore, the risk of having captopril prescribed in a hepatic pathological condition or the hepatotoxicity in long-term use of captopril should be cautioned (37). This study was aimed to explore the effect of captopril on Ca^{2+} homeostasis and cell viability, and to explore their relationship. The HepG2 human hepatoma cell was used in this study because it produces measurable $[Ca^{2+}]_i$ rises upon pharmacological stimulation. It has been shown that in this cell, $[Ca^{2+}]_i$ rises and death can be evoked by stimulation with chemicals such as tamoxifen (21), pyroglutamyl-histidyl-glycine (pEHG) (29) and tectorigenin (19). The Ca^{2+}-sensitive fluorescent dye fura-2 was applied to measure changes in $[Ca^{2+}]_i$. The $[Ca^{2+}]_i$ responses were characterized, the concentration-response relationships were established, the pathways underlying captopril-caused Ca^{2+} influx and Ca^{2+} release were explored.

Materials and Methods

Chemicals

The reagents for cell culture were from Gibco® (Gaithersburg, MD, USA). Aminopolycarboxylic acid/acetoxy methyl (fura-2/AM) and 1,2-bis(2-aminophenoxy)ethane-N,N,N',N'-tetraacetic acid/acetoxy methyl (BAPTA/AM) were from Molecular Probes® (Eugene, OR, USA). All other reagents were from Sigma-Aldrich® (St. Louis, MO, USA) unless otherwise indicated.

Cell Culture

HepG2 human hepatoma cells obtained from Bioresource Collection and Research Center (Taiwan) were cultured in minimum essential medium (MEM) supplemented with 10% heat-inactivated fetal bovine serum, 100 U/ml penicillin and 100 μg/ml streptomycin.

Solutions Used in $[Ca^{2+}]_i$ Measurements

Ca^{2+}-containing medium (pH 7.4) had 140 mM NaCl, 5 mM KCl, 1 mM $MgCl_2$, 2 mM $CaCl_2$,

10 mM 4-(2-hydroxyethyl)-1-piperazineethanesulfonic acid (HEPES), and 5 mM glucose. Ca^{2+}-free medium contained similar chemicals as Ca^{2+}-containing medium except that $CaCl_2$ was replaced with 0.3 mM ethylene glycol tetraacetic acid (EGTA) and 2 mM $MgCl_2$. Captopril was dissolved in absolute alcohol as a 0.1 M stock solution. The other chemicals were dissolved in water, ethanol or dimethyl sulfoxide (DMSO). The concentration of organic solvents in the experimental solutions did not exceed 0.1%, and did not affect viability or basal $[Ca^{2+}]_i$.

$[Ca^{2+}]_i$ Measurements

Confluent cells grown on 6 cm dishes were trypsinized and made into a suspension in culture medium at a concentration of 10^6 cell/ml. Cell viability was determined by trypan blue exclusion. The viability was greater than 95% after the treatment. Cells were subsequently loaded with 2 μM fura-2/AM for 30 min at 25°C in the same medium. After loading, cells were washed with Ca^{2+}-containing medium twice and was made into a suspension in Ca^{2+}-containing medium at a concentration of 10^7 cell/ml. Fura-2 fluorescence measurements were performed in a water-jacketed cuvette (25°C) with continuous stirring; the cuvette contained 1 ml of medium and 0.5 million cells. Fluorescence was monitored with a Shimadzu RF-5301PC spectrofluorophotometer immediately after 0.1 ml cell suspension was added to 0.9 ml Ca^{2+}-containing or Ca^{2+}-free medium, by recording excitation signals at 340 nm and 380 nm and emission signal at 510 nm at 1-s intervals. During the recording, reagents were added to the cuvette by pausing the recording for 2 s to open and close the cuvette-containing chamber. For calibration of $[Ca^{2+}]_i$, after completion of the experiments, the detergent Triton X-100 (0.1%) and $CaCl_2$ (5 mM) were added to the cuvette to obtain the maximal fura-2 fluorescence. Then the Ca^{2+} chelator EGTA (10 mM) was added to chelate Ca^{2+} in the cuvette to obtain the minimal fura-2 fluorescence. Control experiments showed that cells bathed in a cuvette had a viability of 95% after 20 min of fluorescence measurements. $[Ca^{2+}]_i$ was calculated as previously described (17). Mn^{2+} quenching of fura-2 fluorescence was performed in Ca^{2+}-containing medium containing 50 μM $MnCl_2$. $MnCl_2$ was added to cell suspension in the cuvette 30 s before the fluorescence recoding was started. Data were recorded at excitation signal at 360 nm (Ca^{2+}-insensitive) and emission signal at 510 nm at 1-s intervals as described previously (25).

Cell Viability Analyses

The measurement of cell viability was based on the ability of cells to cleave tetrazolium salts by dehydrogenases. Increases in the amount of developed color correlated proportionally with the number of live cells. Assays were performed according to manufacturer's instructions (Roche Molecular Biochemical, Indianapolis, IN, USA). Cells were seeded in 96-well plates at a density of 10^4 cell/well in culture medium for 24 h in the presence of captopril. The cell viability detecting reagent 4-[3-[4-Iodophenyl]-2-4(4-nitrophenyl)-2H-5-tetrazolio-1,3-benzene disulfonate] (water soluble tetrazolium-1, WST-1; 10 μl pure solution) was added to samples after captopril treatment, and cells were incubated for 30 min in a humidified atmosphere. The cells were incubated with/without captopril for 24 h. In the experiments using BAPTA/AM to chelate cytosolic Ca^{2+} to inhibit cytosolic $[Ca^{2+}]_i$ rises, cells were treated with 5 μM BAPTA/AM for 1 h prior to incubation with captopril. The cells were washed once with Ca^{2+}-containing medium and incubated with/without captopril for 24 h. The absorbance of samples (A_{450}) was determined using a multiwall plate reader. Absolute optical density was normalized to the absorbance of unstimulated cells in each plate and expressed as a percentage of the control value. The absorbance of samples (A_{450}) was determined using an enzyme-linked immunosorbent assay (ELISA) reader. Absolute optical density was normalized to the absorbance of unstimulated cells in each plate and expressed as a percentage of the control value.

Statistics

Data are reported as mean ± standard error of the mean (SEM) of three separate experiments. Data were analyzed by one-way analysis of variances (ANOVA) using the Statistical Analysis System (SAS®, SAS Institute Inc., Cary, NC, USA). Multiple comparisons between group means were performed by *post-hoc* analysis using the Tukey's HSD (honestly significantly difference) procedure. A *P*-value less than 0.05 was considered significant.

Results

Effect of Captopril on $[Ca^{2+}]_i$

Fig. 1A shows that the basal $[Ca^{2+}]_i$ level was 51 ± nM. At 500-3000 μM, captopril induced concentration-dependent rises in $[Ca^{2+}]_i$. At a concentration of 3000 μM, captopril induced gradually increasing $[Ca^{2+}]_i$ rises that reached 160 ± 2 nM at 250 s. The response saturated at 3000 μM because 3500 μM captopril did not induce a greater $[Ca^{2+}]_i$.

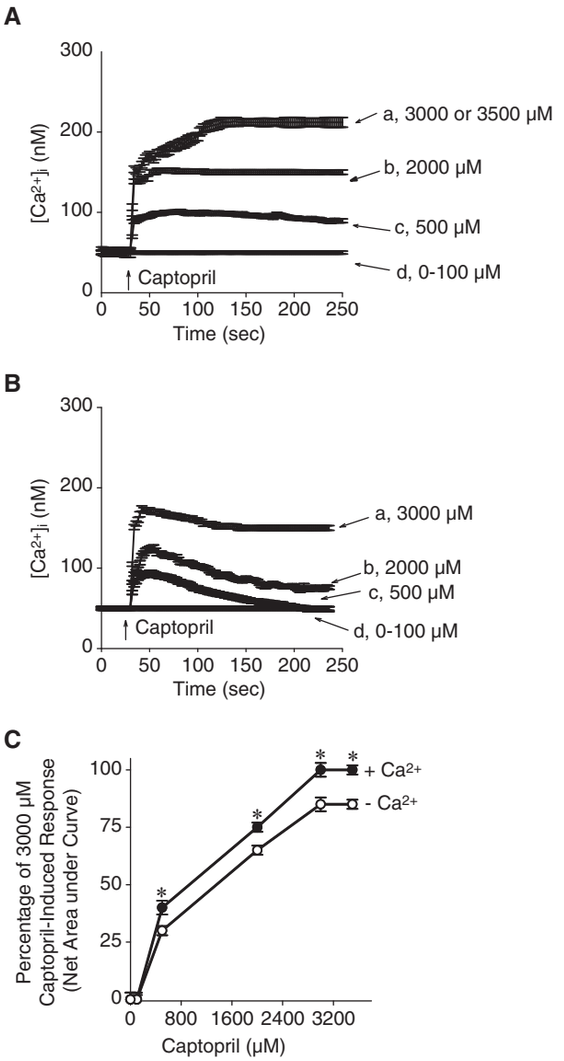

Fig. 1. Effect of captopril on $[Ca^{2+}]_i$ in fura-2-loaded cells. (A) Captopril was added at 25 s. The concentration of captopril was indicated. The experiments were performed in Ca^{2+}-containing medium. Y axis is the $[Ca^{2+}]_i$ induced by captopril in Ca^{2+}-containing medium. (B) Effect of captopril on $[Ca^{2+}]_i$ in the absence of extracellular Ca^{2+}. Captopril was added at 25 s in Ca^{2+}-free medium. Y axis is the $[Ca^{2+}]_i$ rise induced by captopril in Ca^{2+}-free medium. (C) Concentration-response plots of captopril-induced $[Ca^{2+}]_i$ rises in the presence or absence of extracellular Ca^{2+}. Y axis is the percentage of the net (baseline subtracted) area under the curve (25-250 s) of the $[Ca^{2+}]_i$ rises induced by 3000 μM captopril in Ca^{2+}-containing medium. Data are mean ± SEM of three experiments. $*P < 0.05$ compared to open circles.

In Ca^{2+}-free medium, captopril also induced concentration-dependent rises in $[Ca^{2+}]_i$ at 500-3000 μM. At 3000 μM, captopril induced immediate

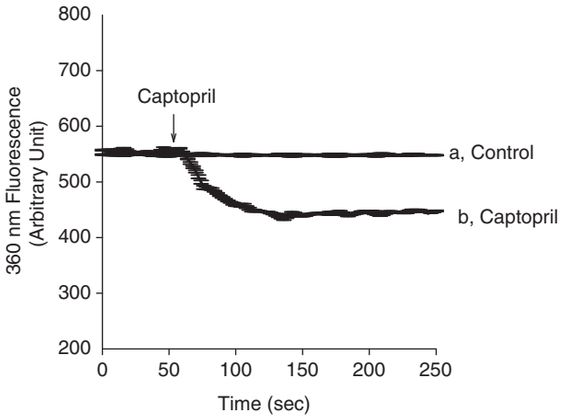

Fig. 2. Effect of captopril on Ca^{2+} influx by measuring Mn^{2+} quenching of fura-2 fluorescence. Experiments were performed in Ca^{2+}-containing medium. $MnCl_2$ (50 μM) was added to cells 1 min before fluorescence measurements. The y axis is fluorescence intensity (in arbitrary units) measured at the Ca^{2+}-insensitive excitation wavelength of 360 nm and the emission wavelength of 510 nm. Trace a: control, without captopril. Trace b: captopril (3000 μM) was added as indicated. Data are mean ± SEM of three separate experiments.

rises in $[Ca^{2+}]_i$ of 130 ± 2 nM followed by a slow decay (Fig. 1B). Fig. 1C shows the concentration-response relationship. The EC_{50} value was 802 ± 5 in Ca^{2+}-containing or 1110 ± 3 nM in Ca^{2+}-free medium, respectively, by fitting to a Hill equation ($P < 0.05$). Ca^{2+} removal reduced the Ca^{2+} signal by approximately 15%.

Captorpil-Induced Mn^{2+} Influx

Mn^{2+} has been shown to enter cells through similar mechanisms as Ca^{2+} but quenches fura-2 fluorescence at all excitation wavelengths (25). Thus this method was used to confirm that captopril-induced $[Ca^{2+}]_i$ rises involved Ca^{2+} influx. The rational is that Ca^{2+} influx could be revealed by quenching of fura-2 fluorescence excited at the Ca^{2+}-insensitive excitation wavelength of 360 nm by Mn^{2+}. Fig. 2 shows that 3000 μM captopril evoked an instant decrease in the 360 nm excitation signal that reached a maximum value of 122 ± 2 arbitrary units at 145 s. This suggests that Ca^{2+} influx participated in captopril-evoked $[Ca^{2+}]_i$ rises.

Regulation of Captopril-Induced $[Ca^{2+}]_i$ Rises

Effort was made to examine the Ca^{2+} influx pathway and the regulation of captopril (3000 μM)-induced Ca^{2+} response (Fig. 3). In Ca^{2+}-containing

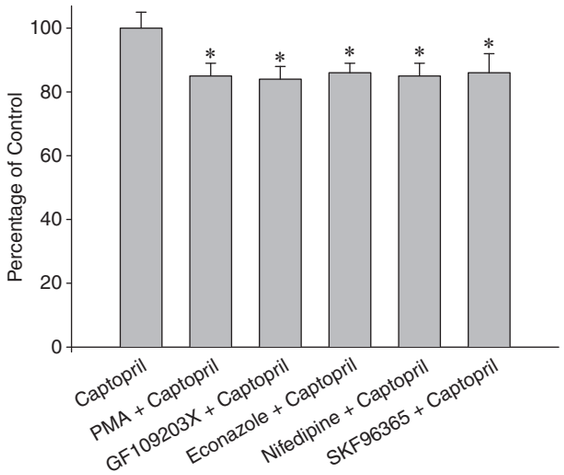

Fig. 3. Effect of Ca^{2+} channel modulators on captopril-induced $[Ca^{2+}]_i$ rises. In blocker- or modulator-treated groups, the reagent was added 1 min before captopril (3000 μM). The concentration was 1 μM for nifedipine, 0.5 μM for econazole, 5 μM for SKF96365, 10 nM for phorbol 12-myristate 13-acetate (PMA), and 2 μM for GF109203X. Data are expressed as the percentage of control (1st column) that is the area under the curve (25-200 s) of 3000 μM captopril-induced $[Ca^{2+}]_i$ rises in Ca^{2+}-containing medium, and are mean ± SEM of three separate experiments. $*P < 0.05$ compared to the 1st column. Data are mean ± SEM of three separate experiments.

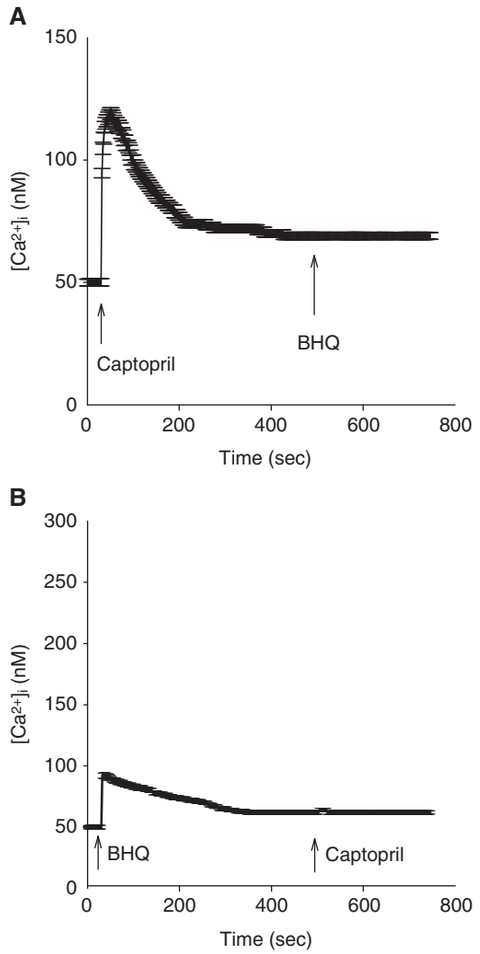

Fig. 4. Effect of BHQ on captopril-induced Ca^{2+} release. (A)(B) BHQ (50 μM) and captopril (3000 μM) were added at time points indicated. Experiments were performed in Ca^{2+}-free medium. Data are mean ± SEM of three separate experiments.

medium, three Ca^{2+} entry inhibitors: nifedipine (1 μM), econazole (0.5 μM) and SKF96365 (5 μM); phorbol 12-myristate 13 acetate (PMA; 1 nM; a protein kinase C, PKC activator); and GF109203X (2 μM; a PKC inhibitor) were applied 1 min before captopril (3000 μM). All these chemicals inhibited captopril-induced $[Ca^{2+}]_i$ rises by approximately 15%. This suggests that store-operated and PKC-regulated Ca^{2+} entry were involved in captopril-induced $[Ca^{2+}]_i$ rises.

Sources of Captopril-Induced Ca^{2+} Release

It has been established that the endoplasmic reticulum is a major Ca^{2+} store in most cell types (3). Thus the role of the endoplasmic reticulum in captopril-caused Ca^{2+} release in HepG2 cells was explored. The experiments were performed in Ca^{2+}-free medium to exclude the contribution of Ca^{2+} influx. Fig. 4A shows that addition of 50 μM 2,5-di-tert-butylhydroquinone (BHQ), an endoplasmic reticulum Ca^{2+} pump inhibitor (27, 35) after treatment with 3000 μM captopril did not cause $[Ca^{2+}]_i$ rises. Fig. 4B shows that after BHQ evoked $[Ca^{2+}]_i$ rises of 52 ± 1 nM, captopril (3000 μM) added afterwards also did not induce $[Ca^{2+}]_i$ rises. This suggests that captopril induced $[Ca^{2+}]_i$ rises by releasing Ca^{2+} from the endoplasmic reticulum.

A Role of Phospholipase C (PLC) in Captopril-Induced $[Ca^{2+}]_i$ Rises

In most cells, PLC is a key enzyme that modulates the release of Ca^{2+} from the endoplasmic reticulum (4). Thus the involvement of PLC in captopril-induced Ca^{2+} release from the endoplasmic reticulum was examined. U73122 is a selective inhibitor of PLC and was used to investigate the role of PLC in captopril-induced Ca^{2+} release (33). First, Fig. 5A

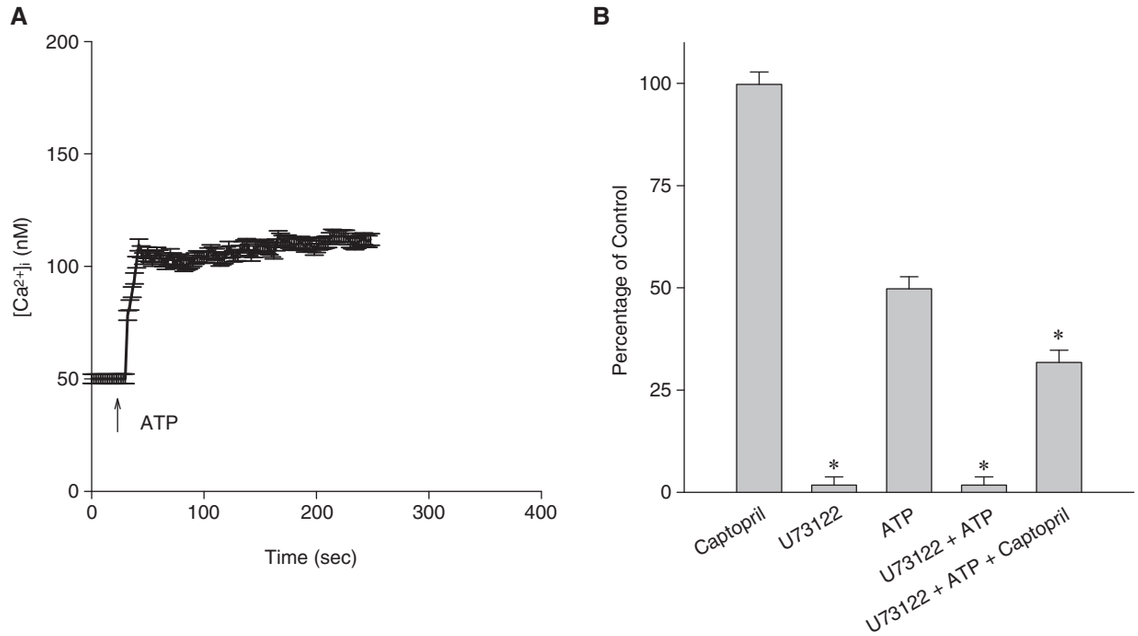

Fig. 5. Effect of U73122 on captopril-induced Ca^{2+} release. Experiments were performed in Ca^{2+}-free medium. (A) ATP (10 μM) was added at 25 s. (B) First column is 3000 μM captopril-induced $[Ca^{2+}]_i$ rises. Second column shows that 2 μM U73122 did not alter basal $[Ca^{2+}]_i$. Third column shows ATP-induced $[Ca^{2+}]_i$ rises. Fourth column shows that U73122 pretreatment for 60 s abolished ATP-induced $[Ca^{2+}]_i$ rises (*$P < 0.05$ compared to 3rd column). Fifth column shows that U73122 (incubation for 60 s) and ATP (incubation for 30 s) pretreatment inhibited 3000 μM captopril-induced $[Ca^{2+}]_i$ rises. Data are mean ± SEM of three experiments.

depicts that ATP (10 μM) induced $[Ca^{2+}]_i$ rises that reached 60 ± 2 nM at 200 s. ATP is a PLC-associated trigger of $[Ca^{2+}]_i$ rises in most cell types (15). Fig. 5B shows that incubation with 2 μM U73122 did not alter basal $[Ca^{2+}]_i$ but abolished ATP-evoked $[Ca^{2+}]_i$ rises. This implies that U73122 fully inhibited PLC activity. The results also show that incubation with 2 μM U73122 inhibited 70% of 3000 μM captopril-induced $[Ca^{2+}]_i$ rises. U73343 is a PLC-insensitive structural analog of U73122 and is often used as a control for U73122 activity. Our data show that U73343 (2 μM) did not alter ATP-evoked $[Ca^{2+}]_i$ rises (not shown). This suggests that U73122 inhibited captopril-induced $[Ca^{2+}]_i$ rises *via* acting on PLC.

Effect of Captopril on Cell Viability

Because $[Ca^{2+}]_i$ rises may regulate viability (4), experiments were conducted to examine the effect of captopril on viability of HepG2 cells. Cells were treated with 0-550 μM captopril for 24 h, and the tetrazolium assay was performed. In the presence of 150-550 μM captopril, cell viability decreased concentration-dependently (Fig. 6).

Lack of an Effect of BAPTA/AM on Reversing Captopril-Induced Cell Death

Another important question was whether the captopril-induced cell death was induced by $[Ca^{2+}]_i$ rises. The intracellular Ca^{2+} chelator BAPTA/AM (34) was applied to prevent $[Ca^{2+}]_i$ rises during captopril treatment. After treatment with 5 μM BAP TA/AM, 3000 μM captopril failed to evoke $[Ca^{2+}]_i$ rises (not shown). This suggests that BAPTA/AM chelated cytosolic Ca^{2+}. Fig. 6 also shows that 5 μM BAPTA/AM loading did not alter the control value of cell viability. In the presence of 150-550 μM captopril, BAPTA/AM loading did not reverse captopril-induced cell death. Therefore, the data suggest that captopril-induced cell death was not caused by preceding rises in $[Ca^{2+}]_i$.

Discussion

In terms of Ca^{2+} signaling, captopril affected Ca^{2+} homeostasis in isolated rat cardiomyocytes (36), aortic smooth muscle (43, 44), and cultured bovine aorta endothelial cells (18). This study represents the first attempt to explore the effect of captopril

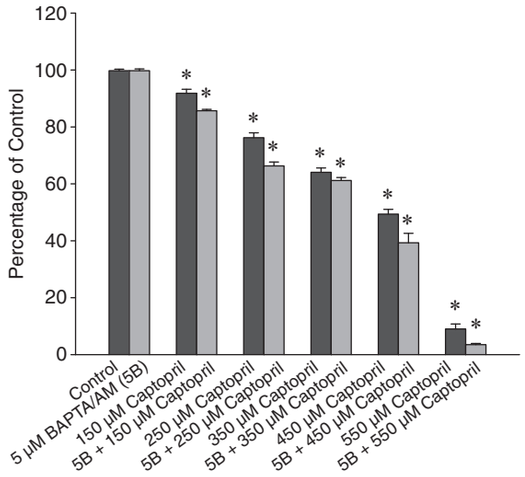

Fig. 6. Cytotoxic effect of captopril. Cells were treated with 0-550 μM captopril for 24 h, and cell viability assay was performed. Data are mean ± SEM of three experiments. Each treatment had six replicates (wells). Data are expressed as percentage of control response that is the increase in cell numbers in captopril-free groups. Control had 10,337 ± 252 cells/well before experiments, and had 13,657 ± 887 cells/well after incubation for 24 h. *$P < 0.05$ compared to control. In each group, the Ca^{2+} chelator BAPTA/AM (5 μM) was added to cells followed by treatment with captopril in medium. Cell viability assay was subsequently performed.

on Ca^{2+} signaling and viability in HepG2 cells. Our study shows that captopril increased $[Ca^{2+}]_i$ in HepG2 cells. The Ca^{2+} signal was composed of Ca^{2+} entry and Ca^{2+} release because the signal was reduced by 15% by removing extracellular Ca^{2+}. The Mn^{2+} quenching data also suggest that Ca^{2+} influx occurred during captopril incubation.

The store-operated Ca^{2+} entry plays a key role in nonexcitable cells (28). In HepG2 cells the dominant Ca^{2+} entry pathway is the store-operated Ca^{2+} channels (7, 32). Our findings show that captopril-evoked $[Ca^{2+}]_i$ rises were inhibited by 15% by econazole, nifedipine, and SKF96365. These three compounds have been used to inhibit store-operated Ca^{2+} entry, although there are so far no selective inhibitors for this entry (8, 10, 14). Therefore, captopril appears to cause Ca^{2+} entry *via* store-operated Ca^{2+} entry.

The activity of many protein kinases can associate with Ca^{2+} signaling. It has been shown that Ca^{2+}-dependent PKC isoforms have specialized roles in short-term synaptic plasticity (6). Conversely, bovine parainfluenza-3 virus selectively depletes a Ca^{2+}-independent, phospholipid-dependent PKC in bovine alveolar macrophages (12). Our data show that captopril-evoked $[Ca^{2+}]_i$ rises were inhibited by 15% by enhancing or inhibiting PKC activity. This suggests that a normally maintained PKC level is needed for captopril to induce a full Ca^{2+} response. The interactive relationship between PKC and store-operated Ca^{2+} entry has been established. Steatosis has been shown to inhibit liver cell store-operated Ca^{2+} entry and reduce endoplasmic reticulum Ca^{2+} through a PKC-dependent mechanism (38). Because 15% of captopril-induced $[Ca^{2+}]_i$ rises was *via* Ca^{2+} influx, this influx appears to involve PKC-regulated store-operated Ca^{2+} entry.

Nifedipine is a L-type voltage-gated Ca^{2+} channel inhibitor, and has some minor effects on voltage-dependent Ca^{2+} channels. In most cases, nifedipine does not affect store-operated Ca^{2+} entry. Although nifedipine may affect store-operated Ca^{2+} entry through the mechanism independent of L-type Ca^{2+} channels in rabbit arteriolar smooth muscle (8), it is not sure how nifedipine affects HepG2 cells. Furthermore, regarding econazole, although previous studies have demonstrated the multiple effects of econazole on store-operated Ca^{2+} entry on other cell types (16, 20), econazole itself is not commonly used as a specific store-operated Ca^{2+} entry inhibitor. Therefore, besides the store-operated and PKC-regulated Ca^{2+} entries, L-type voltage-gated Ca^{2+} channel may be also involved in captopril-induced $[Ca^{2+}]_i$ influx.

Regarding the Ca^{2+} stores involved in captopril-evoked Ca^{2+} release, the BHQ-sensitive endoplasmic reticulum store seemed to be the dominant one. One possible pathway was that captopril acts similarly to BHQ by inhibiting the endoplasmic reticulum Ca^{2+}-ATP pump (27). The data further show that the Ca^{2+} releases was *via* a PLC-dependent mechanism because the release was greatly inhibited (70%) when PLC activity was inhibited. The PLC-independent release may involve other mechanisms such as the phospholipase A2 pathway (28).

PLC is one of the crucial enzymes that modulate the release of Ca^{2+} from the endoplasmic reticulum Ca^{2+} stores *via* the G-protein coupled receptors (GPCR) signaling pathways (3, 4). Because captopril-induced Ca^{2+} releases was *via* a PLC-dependent mechanism, captopril may affect Ca^{2+} homeostasis by activating GPCR signaling pathways in HepG2 cells. Heptahelical GPCR including G-protein coupled Mas receptors have been shown to regulate many vital body functions *via* ACE2/Angiotensin 1-7 (Ang 1-7) (30). A previous study has shown that captopril improved postresuscitation hemodynamics protection against pulmonary embolism by activating the ACE2/Angiotensin 1-7 (Ang 1-7)/G-protein coupled Mas receptor axis (39). In addi-

tion, ACE2/Ang 1-7/G-protein coupled Mas receptor axis has been shown to activate Akt signaling to ameliorate hepatic steatosis in free fatty acid-induced HepG2 cells (5). Therefore, it appears that captopril may induce $[Ca^{2+}]_i$ rises through G-protein coupled Mas receptor-regulated signaling pathway in HepG2 cells.

Previous studies have shown that captopril affected Ca^{2+} homeostasis through different pathways in isolated rat cardiomyocytes (36) and aortic smooth muscles (43, 44). In isolated rat cardiomyocytes, captopril (1-5 μM) decreased $[Ca^{2+}]_i$ rises through voltage-operated Ca^{2+} channels (36). In aortic smooth muscles, captopril (10-20 μM) reduced Ca^{2+} influx *via* PKC-sensitive pathways (43, 44). Our present data show that captopril (500-3000 μM) induced $[Ca^{2+}]_i$ rises by inducing PLC- and PKC-regulated Ca^{2+} release from the endoplasmic reticulum and Ca^{2+} entry *via* store-operated Ca^{2+} channels or L-type voltage-gated Ca^{2+} channels in HepG2 cells. Because various cell types derived from different origins may have different mechanisms of Ca^{2+} homeostasis, depending on the physiological function of this particular cell, it appears that the mechanisms of the effect of captopril on Ca^{2+} homeostasis were different among those models.

A rise in $[Ca^{2+}]_i$ may or may not alter cell viability depending on the agonist and cell type (31). Our results show that captopril caused a Ca^{2+}-independent cell death in a concentration-dependent (150-550 μM) manner. Previous studies have explored the plasma concentration of captopril after oral administration (11, 23). The plasma level of captopril may reach 50 μM. However, in patients with cardiovascular or liver diseases, the plasma concentration of captopril after oral administration might be 10-fold higher than in healthy adults (11, 23). Our data show that captopril at a concentration of 150 μM induced cell death. Thus the potential use of captopril or its derivatives to cope with human hepatoma deserves further exploration in the future.

Viability and $[Ca^{2+}]_i$ assays were different methodology in this study. In viability assays, cells were incubated with captopril for 24 h in order to gain significant changes in viability. Conversely, $[Ca^{2+}]_i$ assays were performed online and terminated within 10 min, and trypan blue exclusion showed that after treatment with captopril for this period of time, cell viability was >95%. This explains 550 μM captopril decreased cell viability by approximately 90% while 3000 μM captopril did not alter viability in $[Ca^{2+}]_i$ assays.

Together, the results show that captopril induced Ca^{2+} influx *via* PKC-sensitive store-operated Ca^{2+} entry and also Ca^{2+} release from the endoplasmic reticulum in a PLC-dependent manner. Captopril also caused Ca^{2+}-independent cell death. Given that Ca^{2+} signaling may affect diverse aspects of cell patho-physiology, the $[Ca^{2+}]_i$-elevating effect and cytotoxicity of captopril should be noted in using this compound for other studies.

Acknowledgments

This work was supported by VGHKS106-102 and VGHKS107-123 to IS Chen; VGHKS107-169 and VGHKS106-151 to CR Jan.

Conflict of Interests

The authors declare that there are no conflicts of interests.

References

1. Andersson, P., Bratt, J., Heimbürger, M., Cederholm, T. and Palmblad, J. Inhibition of neutrophil-dependent cytotoxicity for human endothelial cells by ACE inhibitors. *Scand. J. Immunol.* 80: 339-345, 2014.
2. Attoub, S., Gaben, A.M., Al-Salam, S., Al Sultan, M.A., John, A., Nicholls, M.G., Mester, J. and Petroianu, G. Captopril as a potential inhibitor of lung tumor growth and metastasis. *Ann. N. Y. Acad. Sci.* 1138: 65-72, 2008.
3. Berridge, M.J. Calcium microdomains: organization and function. *Cell Calcium* 40: 405-412, 2006.
4. Bootman, M.D., Lipp, P. and Berridge, M.J. The organisation and functions of local Ca^{2+} signals. *J. Cell Sci.* 114: 2213-2222, 2001.
5. Cao, X., Yang, F., Shi, T., Yuan, M., Xin, Z., Xie, R., Li, S., Li, H. and Yang, J.K. Angiotensin-converting enzyme 2/angiotensin-(1-7)/Mas axis activates Akt signaling to ameliorate hepatic steatosis. *Sci. Rep*. 6: 21592, 2016.
6. Chu, Y., Fioravante, D., Leitges, M. and Regehr, W.G. Calcium-dependent PKC isoforms have specialized roles in short-term synaptic plasticity. *Neuron* 82: 859-871, 2014.
7. Cui, R., Yan, L., Luo, Z., Guo, X. and Yan, M. Blockade of store-operated calcium entry alleviates ethanol-induced hepatotoxicity *via* inhibiting apoptosis. *Toxicol. Appl. Pharmacol.* 287: 52-66, 2015.
8. Curtis, T.M. and Scholfield, C.N. Nifedipine blocks Ca^{2+} store refilling through a pathway not involving L-type Ca^{2+} channels in rabbit arteriolar smooth muscle. *J. Physiol.* 532: 609-623, 2001.
9. De la Iglesia Iñigo, S., López-Jorge, C.E., Gómez-Casares, M.T., Lemes Castellano, A., Martín Cabrera, P., López Brito, J., Suárez Cabrera, A. and Molero Labarta, T. Induction of apoptosis in leukemic cell lines treated with captopril, trandolapril and losartan: a new role in the treatment of leukaemia for these agents. *Leuk. Res.* 33: 810-816, 2009.
10. Dionicio, C.L., Peña, F., Constantino-Jonapa, L.A., Vazquez, C., Yocupicio-Monroy, M., Rosales, R., Zambrano, J.L., Ruiz, M.C., Del Angel, R.M. and Ludert, J.E. Dengue virus induced changes in Ca^{2+} homeostasis in human hepatic cells that favor the viral replicative cycle. *Virus Res.* 245: 17-28, 2017.
11. Duchin, K.L., McKinstry, D.N., Cohen, A.I. and Migdalof, B.H. Pharmacokinetics of captopril in healthy subjects and in patients with cardiovascular diseases. *Clin. Pharmacokinet.* 14: 241-259, 1988.
12. Dyer, R.M., Majumdar, S., Douglas, S.D. and Korchak, H.M.

Bovine parainfluenza-3 virus selectively depletes a calcium-independent, phospholipid-dependent protein kinase C and inhibits superoxide anion generation in bovine alveolar macrophages. *J. Immunol.* 153: 1171-1179, 1994.
13. Fearnley, C.J., Roderick, H.L. and Bootman, M.D. Calcium signaling in cardiac myocytes. *Cold Spring Harb. Perspect. Biol.* 3: a004242, 2011.
14. Finney-Hayward, T.K., Bahra, P., Li, S., Poll, C.T., Nicholson, A.G., Russell, R.E., Ford, P.A., Westwick, J., Fenwick, P.S., Barnes, P.J. and Donnelly, L.E. Leukotriene B4 release by human lung macrophages *via* receptor- not voltage-operated Ca^{2+} channels. *Eur. Respir. J.* 33: 1105-1112, 2009.
15. Florenzano, F., Viscomi, M.T., Mercaldo, V., Longone, P., Bernardi, G. and Bagni, C. P2X2R purinergic receptor subunit mRNA and protein are expressed by all hypothalamic hypocretin/orexin neurons. *J. Com. Neurol.* 498: 58-67, 2006.
16. Gamberucci, A., Fulceri, R., Benedetti, A., and Bygrave, F.L. On the mechanism of action of econazole, the capacitative calcium inflow blocker. *Biochem. Biophys. Res. Commun.* 248: 75-77, 1998.
17. Grynkiewicz, G., Poenie, M. and Tsien, R.Y. A new generation of Ca^{2+} indicators with greatly improved fluorescence properties. *J. Biol. Chem.* 260: 3440-3450, 1985.
18. Hirano, K., Hirano, M. and Kanaide, H. Enhancement by captopril of bradykinin-induced calcium transients in cultured endothelial cells of the bovine aorta. *Eur. J. Pharmacol.* 244: 133-137, 1993.
19. Jiang, C.P., Ding, H., Shi, D.H., Wang, Y.R., Li, E.G. and Wu, J.H. Pro-apoptotic effects of tectorigenin on human hepatocellular carcinoma HepG2 cells. *World J. Gastroenterol.* 18: 1753-1764, 2012.
20. Jan, C.R., Ho, C.M., Wu, S.N. and Tseng, C.J. Multiple effects of econazole on calcium signaling: depletion of thapsigargin-sensitive calcium store, activation of extracellular calcium influx, and inhibition of capacitative calcium entry. *Biochim. Biophys. Acta* 1448: 533-542, 1999.
21. Kim, J.A., Kang, Y.S., Jung, M.W., Lee, S.H. and Lee, Y.S. Involvement of Ca^{2+} influx in the mechanism of tamoxifen-induced apoptosis in HepG2 human hepatoblastoma cells. *Cancer Lett.* 147: 115-123, 1999.
22. Li, T., Zhou, R., Yao, Y., Yang, Q., Zhou, C., Wu, W., Li, Q., You, Z., Zhao, X., Yang, L., Li, C., Zhu, D., Qiu, Y., Luo, M., Tan, Z., Li, H., Chen, Y., Gong, G., Feng, Y., Dian, K. and Liu, J. Angiotensin-converting enzyme inhibitor captopril reverses the adverse cardiovascular effects of polymerized hemoglobin. *Antioxid. Redox. Signal.* 21: 2095-2108, 2014.
23. Mandal, A.S., Chatterjee, S., Kundu, S., Biswas, N., Guha, A., Paul, S. and Kuotsu, K. *In vitro-in vivo* correlation and bioavailability studies of captopril from novel controlled release donut shaped tablet. *Int. J. Pharm.* 421: 145-150, 2011.
24. Marampon, F., Gravina, G.L., Scarsella, L., Festuccia, C., Lovat, F., Ciccarelli, C., Zani, B.M., Polidoro, L., Grassi, D., Desideri, G., Evangelista, S. and Ferri, C. Angiotensin-converting-enzyme inhibition counteracts angiotensin II-mediated endothelial cell dysfunction by modulating the p38/SirT1 axis. *J. Hypertens.* 31: 1972-1983, 2013.
25. Merritt, J.E., Jacob, R. and Hallam, T.J. Use of manganese to discriminate between calcium influx and mobilization from internal stores in stimulated human neutrophils. *J. Biol. Chem.* 264: 1522-1527, 1989.
26. Meyers, R.S. and Siu, A. Pharmacotherapy review of chronic pediatric hypertension. *Clin. Ther.* 33: 1331-1356, 2011.
27. Muallem, S., Loessberg, P., Sachs, G. and Wheeler, L.A. Agonist-sensitive and -insensitive intracellular Ca^{2+} pools. Separate Ca^{2+}-releasing mechanisms revealed by manoalide and benzohydroquinone. *Biochem. J.* 279: 367-375, 1991.
28. Putney, J.W. Jr. A model for receptor-regulated calcium entry. *Cell Calcium* 7: 1-12, 1986.
29. Reichelt, W.H., Iversen, J.G., Paulsen, J.E., Elgjo, K. and Reichelt, K.L. Pyroglutamyl-histidyl-glycine, the endogenous colon mitosis inhibitor, regulates cyclic AMP level in non-tumorigenic colonic epithelial cells. *Anticancer Res.* 24: 1465-1468, 2004.
30. Solinski, H.J., Gudermann, T. and Breit, A. Pharmacology and signaling of MAS-related G protein-coupled receptors. *Pharmacol. Rev.* 66: 570-597, 2014.
31. Stueber, T., Eberhardt, M.J., Caspi, Y., Lev, S., Binshtok, A. and Leffler, A. Differential cytotoxicity and intracellular calcium-signalling following activation of the calcium-permeable ion channels TRPV1 and TRPA1. *Cell Calcium* 68: 34-44, 2017.
32. Sun, D.P., Li, X.X., Liu, X.L., Zhao, D., Qiu, F.Q., Li, Y. and Ma, P. Gypenosides induce apoptosis by Ca^{2+} overload mediated by endoplasmic-reticulum and store-operated Ca^{2+} channels in human hepatoma cells. *Cancer Biother. Radiopharm.* 28: 320-326, 2013.
33. Thompson, A.K., Mostafapour, S.P., Denlinger, L.C., Bleasdale, J.E. and Fisher, S.K. The aminosteroid U-73122 inhibits muscarinic receptor sequestration and phosphoinositide hydrolysis in SK-N-SH neuroblastoma cells. A role for Gp in receptor compartmentation. *J. Biol. Chem.* 266: 23856-23862, 1991.
34. Tsien, R.Y. New calcium indicators and buffers with high selectivity against magnesium and protons: design, synthesis, and properties of prototype structures. *Biochemistry* 19: 2396-2404, 1980.
35. Van Esch, G.J. Toxicology of tert-butylhydroquinone (TBHQ). *Food Chem. Toxicol.* 24: 1063-1065, 1986.
36. Wang, J., Zhang, L., Qi, J.H., Zhang, P.J., Wei, P.J., Gu, P.K. and Jin, Z.J. Effects of captopril and enalaprilat on intracellular Ca^{2+} content in isolated cardiomyocytes from rats. *Zhongguo Yao Li Xue Bao* 17: 233-235, 1996.
37. Wengrower, D., Zanninelli, G., Pappo, O., Latella, G., Sestieri, M., Villanova, A., Faitelson, Y., Pines, M. and Goldin, E. Prevention of fibrosis in experimental colitis by captopril: the role of tgf-beta1. *Inflamm. Bowel Dis*. 10: 536-545, 2004.
38. Wilson, C.H., Ali, E.S., Scrimgeour, N., Martin, A.M., Hua, J., Tallis, G.A., Rychkov, G.Y. and Barritt, G.J. Steatosis inhibits liver cell store-operated Ca^{2+} entry and reduces ER Ca^{2+} through a protein kinase C-dependent mechanism. *Biochem. J.* 466: 379-390, 2015.
39. Xiao, H.L., Li, C.S., Zhao, L.X., Yang, J., Tong, N., An, L. and Liu, Q.T. Captopril improves postresuscitation hemodynamics protective against pulmonary embolism by activating the ACE2/Ang-(1-7)/Mas axis. *Naunyn Schmiedebergs Arch. Pharmacol.* 389: 1159-1169, 2016.
40. Yu, W., Akishita, M., Xi, H., Nagai, K., Sudoh, N., Hasegawa, H., Kozaki, K. and Toba, K. Angiotensin converting enzyme inhibitor attenuates oxidative stress-induced endothelial cell apoptosis *via* p38 MAP kinase inhibition. *Clin. Chim. Acta* 364: 328-334, 2006.
41. Yun, B., Lee, H., Ewing, H., Gelb, M.H. and Leslie, C.C. Off-target effect of the cPLA2α inhibitor pyrrophenone: Inhibition of calcium release from the endoplasmic reticulum. *Biochem. Biophys. Res. Commun.* 479: 61-66, 2016.
42. Zagariya, A., Bhat, R., Navale, S., Chari, G. and Vidyasagar, D. Inhibition of meconium-induced cytokine expression and cell apoptosis by pretreatment with captopril. *Pediatrics* 117: 1722-1727, 2006.
43. Zhu, Z., Tepel, M., Neusser, M., Mehring, N. and Zidek, W. Effect of captopril on vasoconstriction and Ca^{2+} fluxes in aortic smooth muscle. *Hypertension* 22: 806-811, 1993.
44. Zhu, Z., Tepel, M., Neusser, M. and Zidek, W. Mechanism of the action of angiotensin-converting enzyme inhibitors on agonist-induced Ca^{2+} influx. *J. Vasc. Res.* 31: 265-270, 1994.